Proc. Natl. Acad. Sci. USA
Vol. 93, pp. 12327–12332, October 1996
Cell Biology

Real time observation of anaphase *in vitro*

ANDREW W. MURRAY*†‡§, ARSHAD B. DESAI*‡, AND E. D. SALMON*¶

*Marine Biological Laboratory, Woods Hole, MA 02453; Departments of †Physiology and ‡Biochemistry, University of California, San Francisco, CA 94143; and ¶Department of Biology, University of North Carolina, Chapel Hill, NC 27599

Communicated by Shinya Inoué, Marine Biological Laboratory, Woods Hole, MA, June 18, 1996 (received for review April 15, 1996)

ABSTRACT **We used digital fluorescence microscopy to make real-time observations of anaphase chromosome movement and changes in microtubule organization in spindles assembled in *Xenopus* egg extracts. Anaphase chromosome movement in these extracts resembled that seen in living vertebrate cells. During anaphase chromosomes moved toward the spindle poles (anaphase A) and the majority reached positions very close to the spindle poles. The average rate of chromosome to pole movement (2.4 μm/min) was similar to earlier measurements of poleward microtubule flux during metaphase. An increase in pole-to-pole distance (anaphase B) occurred in some spindles. The polyploidy of the spindles we examined allowed us to observe two novel features of mitosis. First, during anaphase, multiple microtubule organizing centers migrated 40 μm or more away from the spindle poles. Second, in telophase, decondensing chromosomes often moved rapidly (7–23 μm/min) away from the spindle poles toward the centers of these asters. This telophase chromosome movement suggests that the surface of decondensing chromosomes, and by extension those of intact nuclei, bear minus-end-directed microtubule motors. Preventing the inactivation of Cdc2/cyclin B complexes by adding nondegradable cyclin B allowed anaphase A to occur at normal velocities, but reduced the ejection of asters from the spindles, blocked chromosome decondensation, and inhibited telophase chromosome movement. In the presence of nondegradable cyclin B, chromosome movement to the poles converted bipolar spindles into pairs of independent monopolar spindles, demonstrating the role of sister chromatid linkage in maintaining spindle bipolarity.**

The orderly segregation of chromosomes at mitosis has fascinated cell biologists for more than 100 years (1). What are the components of the spindle, how do they interact with each other to produce a reproducible yet highly dynamic structure, and how do the activities that regulate the cell cycle sequentially induce formation of the spindle and chromosome segregation? The ultimate answer to these questions will require assembling functional spindles from purified components and studying how defined molecules regulate spindle behavior. This paper presents a step toward this goal: real-time observations of anaphase in spindles assembled in a test tube.

Analyzing mitosis in tissue culture cells and early embryos has revealed the dynamic behavior of the microtubules that comprise the spindle and their interactions with the kinetochores, the specialized regions that attach chromosomes to the spindle (reviewed in ref. 2). Studies on frog eggs identified maturation promoting factor (MPF) as the activity that induced mitosis and meiosis, and showed that MPF was an active protein kinase composed of Cdc2 complexed to cyclin B (reviewed in ref. 3). The proteolysis of cyclin B inactivates MPF, inducing chromosome decondensation, nuclear envelope formation, and changes in microtubule dynamics that convert the short dynamic microtubules of the metaphase spindle into the long, relatively stable microtubules of interphase cells (2, 4–7). Inactivating MPF destroys interactions between microtubules and chromatin (8) and this change is believed to contribute to the disassembly of the spindle and the formation of interphase asters, circularly symmetric arrays of microtubules that are nucleated at the center of the array.

Extracts of frog eggs can recapitulate the cell cycle *in vitro* (9–11) and assemble functional spindles. Experiments on spindle behavior (4, 10, 12, 13) exploit the natural cell cycle arrest of unfertilized frog eggs, which are held in metaphase of meiosis II by the activity cytostatic factor (CSF), the product of the *c-mos* protooncogene (14). At fertilization, an increase in the cytoplasmic calcium concentration overcomes the action of CSF, triggering the destruction of cyclin B and the onset of anaphase (15). In extracts, the addition of exogenous calcium mimics fertilization, and analyzing fixed samples has shown that sister chromatid separation requires the activity of topoisomerase II (4) and depends on the ubiquitin-mediated proteolysis of proteins other than cyclin B (5).

We present real-time observations of changes in microtubule organization and chromosome movements as extracts are induced to proceed from metaphase, through anaphase, and into interphase. The rate and extent of anaphase A movement in these preparations is independent of the destruction of cyclin B and the inactivation of MPF. The polyploid spindles we have observed expel multiple asters during the metaphase to anaphase transition without compromising the orderly movement of the condensed chromosomes to their spindle poles. In telophase, the decondensing chromosomes move rapidly, often over many micrometers, toward the centers of the expelled asters. Preventing MPF inactivation suppresses both aster expulsion and telophase chromosome movement.

MATERIALS AND METHODS

Slide and Extract Preparation. Slides and coverslips were successively washed with distilled water, ethanol, and acetone. Slides were coated with latex beads: 30 μl of a 100-fold dilution of 12 μm diameter latex beads (Sigma) in ethanol were spread on the surface of a slide and allowed to air dry. This procedure yields a density of beads that maintains separation between slide and coverslip without interfering with spindle observation.

Spindles were prepared using CSF-arrested extracts from *Xenopus* eggs (4) and induced to enter anaphase by adding $CaCl_2$ to 0.3 mM. Immediately after calcium addition, 4 μl of the extract was placed on a glass slide that had been coated with 12-μm-diameter latex beads, and an 18 × 18 mm coverslip was gently placed on top of the drop. The preparation was sealed by flowing a 2:1 mixture of trichlorotrifluoroethane (Aldrich)/halocarbon oil (Halocarbon Products, Hackensack, NJ), around the perimeter of the extract. The induction of anaphase in the presence of nondegradable cyclin B (cyclin

The publication costs of this article were defrayed in part by page charge payment. This article must therefore be hereby marked "*advertisement*" in accordance with 18 U.S.C. §1734 solely to indicate this fact.

Abbreviations: MPF, maturation promoting factor; CSF, cytostatic factor; DAPI, 4′,6′-diamidino-2-phenylindole.

§To whom reprint requests should be addressed at: Physiology Box 0444, University of California, San Francisco, CA 94143-0444. e-mail: amurray@cgl.ucsf.edu.

B-Δ90) has been described (5). Cyclin B-Δ90 was added at least 40 min after the addition of CSF and 20–30 min before calcium was added to induce anaphase.

Microscopy and Data Analysis. A digital epifluorescence microscope was constructed for these experiments (16). We visualized DNA by including 4′,6′-diamidino-2-phenylindole (DAPI) at 0.05 μg/ml, and the microtubules were visualized by supplementing the extracts with 50–100 μg/ml of tetramethylrhodamine-labeled tubulin (13). Fluorescent images of chromosomes and spindles were recorded in time-lapse by epifluorescence microscopy using a Nikon FX-A microscope, with a ×20, NA = 0.75 lens and a Hamamatsu C4880 cooled charge-coupled device camera (Hamamatsu Photonics, Middlesex, NJ) operated in the super high gain mode for a 300 × 300 pixel, 12-bit deep central region of the detector. At 30- or 60-sec intervals, DAPI, rhodamine, and sometimes phase contrast digital images, exposed for 600 msec, were recorded into separate image stacks within a Metamorph digital imaging computer (Universal Image, West Chester, PA). A multiple bandpass dichromatic epifluorescent filter and multiple excitation and neutral density filter wheels were used to control illumination wavelength and intensity. The camera, shutters for epi- and transillumination, and the filter wheels were all controlled by Metamorph. Changes in spindle fluorescence intensity, chromosome movements, and aster dynamics were quantified by using morphometric analysis algorithms in Metamorph in combination with spreadsheet analysis (Microsoft EXCEL). Photographs were prepared using Adobe PHOTOSHOP, labeled in CLARIS DRAW, and printed on a Tektronics Phaser dye sublimation printer.

RESULTS

We examined the transition from metaphase to anaphase in frog egg extracts by real time digital fluorescence microscopy. The extracts were supplemented with rhodamine-labeled tubulin and the DNA-binding dye DAPI to visualize microtubules and chromosomes. Metaphase spindles were prepared by a two step procedure. Sperm nuclei were added to a CSF-arrested extract, and calcium was added to induce the inactivation of MPF and formation of interphase nuclei. The extracts were incubated for 80 min to allow DNA replication, centrosome duplication, and the sequestration of the added calcium into membrane-bound compartments (17). More CSF-arrested extract was then added to induce nuclear envelope breakdown and spindle assembly (4). The spindles were induced to enter anaphase by adding exogenous calcium to induce the ubiquitin-dependent proteolysis of cyclin B and unknown proteins that are required to maintain the linkage between sister chromatids (4, 5). Immediately after calcium addition, a portion of the extract was transferred to a microscope slide, sealed with a layer of halocarbon oil, and observed by epifluorescent microscopy with a cooled charge-coupled device camera. We collected paired images of the rhodamine-labeled microtubules and the DAPI-stained DNA at 30-sec intervals for a period of about 30 min.

Anaphase Chromosome Movement. Fig. 1*A* shows a series of images from a typical spindle proceeding through anaphase and into interphase (times are indicated in minutes after the onset of anaphase). This spindle, like the majority of those in the extracts, had more chromosomes than an individual sperm, was probably formed from the contents of several sperm nuclei and thus contained multiple centrosomes (13). The pulse of calcium initiated the following changes: the ejection of asters from the spindle, the separation of sister chromatids, anaphase A and anaphase B, splaying outward of the half-spindles, decreasing microtubule density in the spindle, and in telophase, the rapid movement of decondensing chromosomes toward the centers of expelled asters. These changes are described in more detail below.

Shortly before anaphase chromosome movement started, asters began to migrate away from several different sites near and along the ends of the barrel-shaped spindles, and these microtubule-organizing centers continued to move away from the spindle throughout anaphase (Figs. 1*A* and 2*A*). We also observed asters near, but clearly separated from, the poles of anaphase spindles in samples fixed from reactions in test tubes. This strongly suggests that astral expulsion is not restricted to spindles between a slide and coverslip. The number of asters expelled was roughly correlated with the width of the spindle and reached a maximum of about 16 per spindle. The average rate of astral movement away from their exit site in the spindle was 4.3 μm/min over an average distance of 43 μm (Table 1). The speed of expulsion remained roughly constant as the asters moved away from the spindle, suggesting that the forces acting on the asters do not change as the separation between the asters and the remainder of the spindle increases (data not shown).

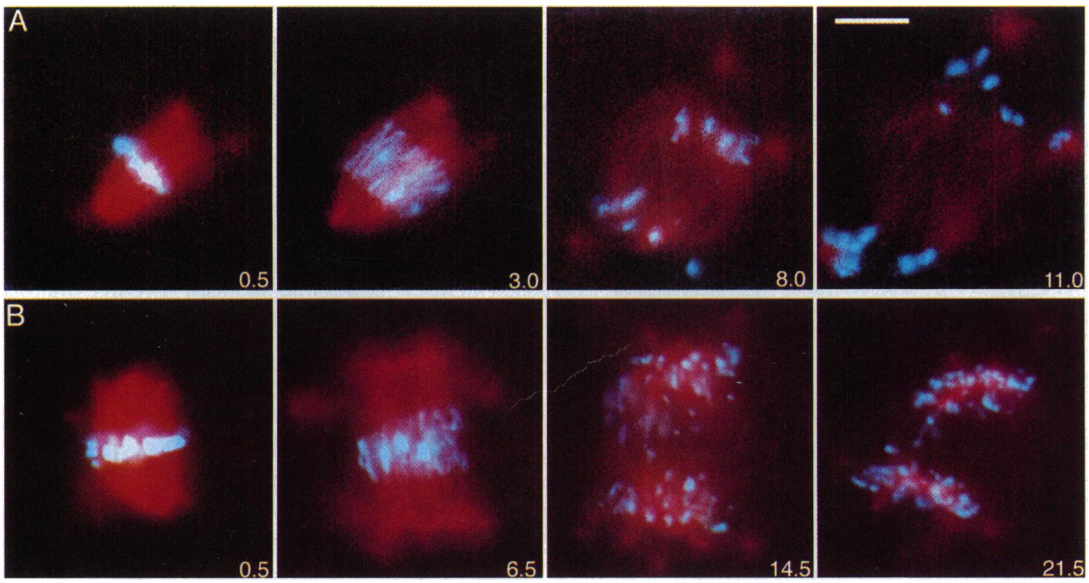

FIG. 1. Anaphase chromosome movements and spindle dynamics *in vitro*. Rhodamine-labeled microtubules are shown in red while DAPI labeled chromosomes are shown in blue green. Time is given in minutes after the onset of anaphase. (*A*) Anaphase in a control extract. (*B*) Anaphase in an extract with added cyclin B-Δ90. (Bar = 20 μm.)

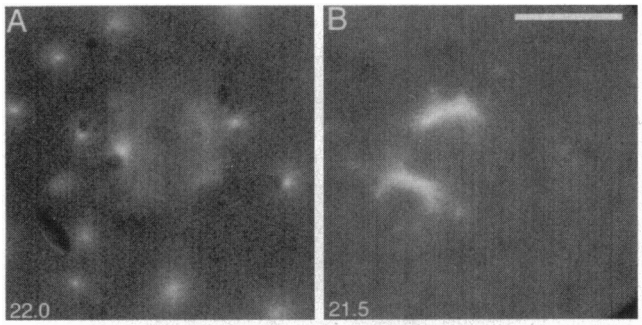

FIG. 2. Astral ejection (*A*, control) and cyclin B-Δ90-treated spindles (*B*). In *A*, the large dark regions are the latex beads and the small dark regions are telophase chromosomes. In the control spindle, the asters grew large by late anaphase; many have already moved beyond the field of view. With cyclin B-Δ90, ejection of tiny dim asters occurs over short distances. Time is given in min after onset of anaphase. (Bar = 20 μm.)

During anaphase, chromosomes moved directly toward the ends of the spindle along paths parallel to the long axis of the spindle and were not attracted by any of the asters that had left the spindle (Figs. 1*A* and 3*A*). During this movement, a specific part of the chromosome, which we presume to be the kinetochore, led the movement toward the spindle pole. The observation that the paths of the chromosomes do not converge to a point as they approach the end of the spindle suggests that the functional spindle poles are distributed structures that lie along the two ends of the barrel-shaped spindles. Within a given spindle the rate of anaphase A showed little variation among chromosomes, and the variation among a population of spindles was small (average rate = 2.4 ± 1.0 μm/min; Table 1). The extent of anaphase B was extremely variable, with some spindles showing no increase in pole to pole separation and others showing a 50% increase in the length of the spindle (Fig. 3*A* and Table 1).

In telophase of mitosis in early embryos, individual chromosomes acquire an intact nuclear envelope as they decondense (18). We monitored this process by the conversion of elongated chromosomes into roughly spherical structures that excluded the background fluorescence of unpolymerized rhodamine tubulin. As they formed, telophase chromosomes became capable of moving rapidly (15 ± 6 μm/min; Table 1) and over long distances (as much as 23 μm) toward the centers of expelled asters and in some cases could be seen to alternate between moving toward two different aster centers (see three marked telophase chromosomes on Fig. 4). As the individual telophase chromosomes approached an aster they fused with each other to form an interphase nucleus.

Anaphase in the Presence of Nondegradable Cyclin B. Since MPF has been reported to control the dynamic behavior of microtubules (6, 7), we studied spindles undergoing anaphase

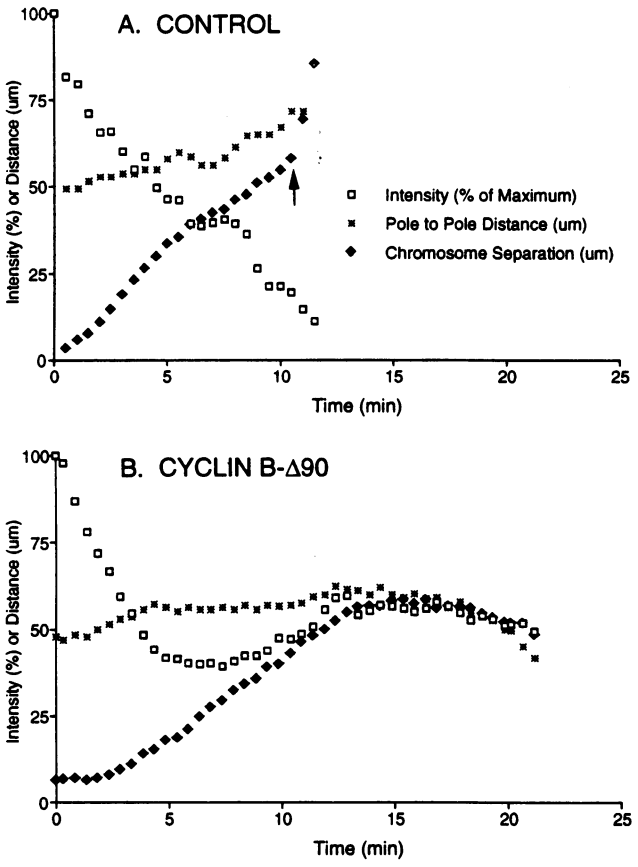

FIG. 3. Anaphase kinetics of chromosome separation, spindle pole elongation and spindle assembly without (*A*) and with (*B*) added cyclin-B Δ90. Chromosome separation was measured as the distance (in μm) between the leading edges of separating sister chromatids. Microtubule density was measured as the percentage of initial intensity in the rhodamine channel at a location midway between the metaphase position of the chromosomes and the poles. Time is given in minutes after the onset of anaphase. The arrow in *A* marks the onset of telophase chromosome movement. In *B*, the interpolar distance shortened in late anaphase because the two half-spindles were pushed closer together by flow in the cytoplasmic extract.

in the presence of cyclin B-Δ90, which cannot be degraded and thus prevents the inactivation of MPF (19). The addition of calcium to these spindles induced anaphase chromosome movement, whose rate and extent was not significantly different from that of control spindles (Figs. 1*B* and 3*B* and Table 1). When the chromosomes reached the spindle poles, however, they did not decondense or show movements toward any of the asters that had been expelled from the spindles. These

Table 1. The effect of cyclin-B Δ90 on anaphase movements

Movement	Added cyclin	Velocity,* μm/min	Distance,* μm	Measurements
Anaphase A†	None	2.4 ± 1.0	21 ± 9	11
	Cyclin-B Δ90	1.9 ± 0.7	22 ± 7	8
Anaphase B	None	1.6 ± 1.4	13 ± 10	5
	Cyclin-B Δ90	2.0 ± 1.1	15 ± 7	4
Telophase chromosome	None	15 ± 6	18 ± 10	14
Motility	Cyclin-B Δ90	0	0	
Aster ejection	None	4.4 ± 2.0	45 ± 31	15
	Cyclin-B Δ90	1.6 ± 1.6	12 ± 6	13

*Average ± SD.

†Anaphase A velocities were obtained from measurements of either chromosome to pole movement directly or by subtracting the contribution of pole to pole elongation from the kinetics of measurements of sister chromatid separation (Fig. 3).

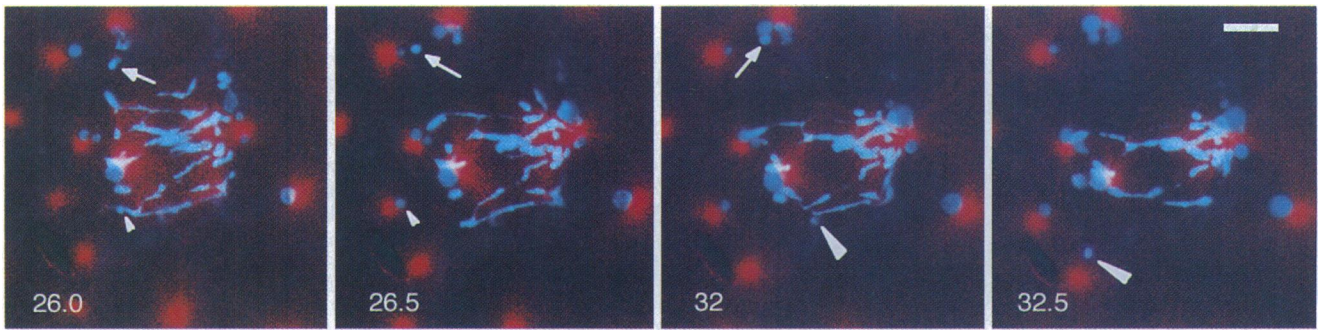

FIG. 4. Telophase chromosome movements toward aster centers in a control spindle preparation with multiple ejected asters as described in the legend to Fig. 2*A*. Pseudocolor is as described for Fig. 1, except the intensity in the rhodamine image has been enhanced to show the weak fluorescence of the telophase asters. Time is given in minites after the onset of anaphase. Note that the upper telophase chromosome marked by the arrow moves first to the center of the left aster then later to the right aster. The middle telophase chromosome marked by the small arrowhead moves to the left center. The lower telophase chromosome marked by a large arrowhead moves toward a lower aster center. (Bar = 20 μm.)

results extend earlier studies (5, 20) which showed that MPF inactivation is not required for chromosome segregation, although it is essential for chromosome decondensation and nuclear envelope reformation.

The behavior of the spindle microtubules in the presence of cyclin B-Δ90 differed in three other respects from that seen in control extracts. (*i*) Although aster ejection still occurred in the presence of cyclin B-Δ90, the rate of aster ejection was only one-third of that seen in control spindles and the average ejection distance was much shorter (Table 1). Both of these differences are statistically significant ($P \leq 0.001$ in the paired *t* test). (*ii*) The asters in extracts containing cyclin B-Δ90 remained tiny in comparison to the asters expelled in control extracts (compare Fig. 2 *A* and *B*). (*iii*) In the regions between the spindle poles and the chromosomes moving toward them, the microtubule density fell more slowly in extracts containing cyclin B-Δ90 (compare Fig. 3 *A* and *B*).

In cyclin B-Δ90-treated extracts, the decline in microtubule density differed greatly between two types of spindles. In most spindles, the great majority of chromosomes segregated successfully and the microtubule density at the site of the former metaphase plate dropped to undetectable levels (see Fig. 1*B*). Even in those spindles that lacked anaphase B, this loss converted the spindles into two apparently independent half spindles, each of whose length was less than half that of the original metaphase spindle. In a minority of spindles a significant fraction of the chromosomes failed to segregate from each other. When this happened, the density of microtubules near the metaphase plate stayed high, and the spindle remained a single bipolar structure, even though about half the chromosomes segregated normally to the poles (Fig. 5). This observation implies that chromosomes stabilize the interactions between antiparallel microtubules that occur near the metaphase plate. We do not know why some spindles, with or without cyclin B-Δ90, fail to segregate all their chromosomes. Possibilities include failures in chromosome replication or condensation, or physical interactions between the nonsegregating chromosomes and the glass of the slide or coverslip.

DISCUSSION

We used digital fluorescence microscopy to follow the progress of anaphase in frog egg extracts. Most aspects of spindle behavior in these extracts closely parallel those seen in real cells, but we have also observed two novel phenomena: the expulsion of microtubule asters from the spindle during anaphase, and a novel form of microtubule-mediated motility shown by telophase chromosomes. Preventing the inactivation of MPF has no effect on anaphase A, reduces aster ejection and the fall in microtubule density seen between the spindle pole and the advancing chromosomes, and completely blocks the fast telophase chromosome movement.

Anaphase Aster Ejection. Aster expulsion during anaphase helps to clarify the relationship between spindle poles and other microtubule-organizing centers. The spindles we observed probably arose by side-to-side fusion of multiple spindles, each containing a pair of centrosomes (13). Thus the expelled asters are likely centrosomes, although we cannot exclude the possibility that they are centriole-free microtubule organizing centers like those assembled in taxol-treated frog egg extracts (21).

Whatever their source, these extra asters are clearly functionally different from the spindle poles in anaphase: the departing asters do not grossly affect the organization of microtubules within the spindle, and as long as chromosomes stay condensed they are not attracted to the migrating asters. This observation is consistent with other demonstrations that spindles poles are specialized structures that can function in the absence of centrosomes (22, 23), although we do not know whether the spindle poles we observed retain any functional centrosomes. Examining diploid spindles in lysed eggs shows that microtubule asters (which presumably contain the centrosome) can be detached from mitotic spindles without

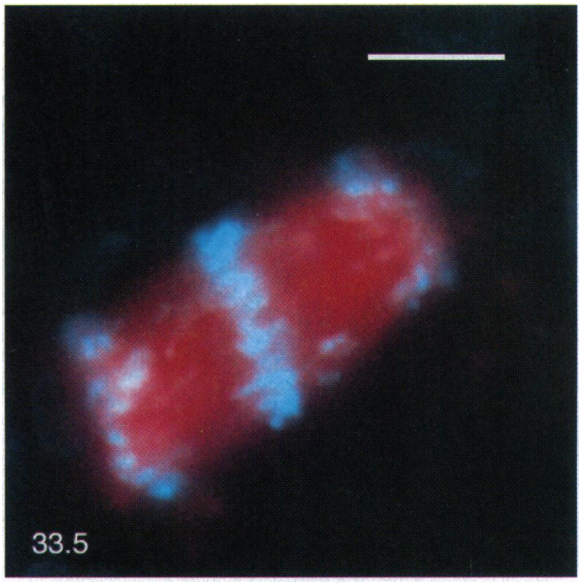

FIG. 5. The role of chromosomes in maintaining spindle integrity demonstrated by a cyclin B-Δ90-treated spindle with stuck chromosomes in late anaphase. Pseudocolor is the same as described in the legend for Fig. 1. Time is given in minutes after onset of anaphase. (Bar = 20 μm.)

affecting anaphase spindle organization or chromosome segregation (unpublished results). Perhaps the primary role of the centrosomes is to nucleate the array of microtubules that captures the kinetochores early in mitosis. As mitosis progresses, the interaction of these kinetochore microtubules with each other and with other components of the spindle may create a spindle pole that can function after removal of the centrosome.

Telophase Chromosome Movement. At the end of anaphase, we saw chromosomes decondense and make rapid movements toward any nearby aster, often moving first toward one and then toward another. This movement is hard to see in telophase tissue culture cells whose chromosomes decondense collectively to form an interphase nucleus associated with a single aster. In early embryonic cells, the decondensing chromosomes form telophase chromosomes by acquiring a nuclear envelope before they fuse with each other to form a single nucleus (18). In our experiments, the presence of extra asters revealed the differences between the movements of telophase chromosomes and condensed mitotic chromosomes. Two observations suggest that aster-directed movement requires a nuclear envelope: movement does not start until the telophase chromosomes exclude the fluorescence of unpolymerized tubulin, and chromosomes in extracts containing nondegradable cyclin do not decondense or exhibit this movement. Perhaps aster directed-movement is due to association between the nuclear envelope and a minus-end directed microtubule motor, such as cytoplasmic dynein (24) or Kar3 (25). In a daughter cell with a single aster, a nuclear envelope-associated motor would move the telophase chromosomes to the center of the aster, inducing them to fuse into a single interphase nucleus. Minus-end-directed motors on the nuclear envelope could also explain the migration of the female pronucleus toward the center of the sperm aster in fertilized eggs (26).

MPF and Anaphase. We used nondegradable cyclin B to ask what aspects of anaphase required the inactivation of MPF. Sister chromatid separation, anaphase A, and anaphase B, all occurred normally, confirming that these events are independent of MPF inactivation (5, 20). In contrast, three other events were affected by adding nondegradable cyclin: chromosomes did not decondense, the expelled asters were smaller and moved away from the spindle more slowly, and there was a smaller fall in the microtubule density between the advancing chromosomes and the spindle poles. These events are normally induced by the effects of MPF on microtubule dynamics (6, 7), the activity and localization of microtubule motors (27, 28), and the ability of chromatin to stabilize microtubules (29). Inactivating MPF increases the average length of microtubules but decreases the number of microtubules generated by a centrosome (30). For free asters, this increase in length would allow microtubule-dependent forces (generated by microtubule motors or polymerization) to move the asters more rapidly. At the spindle poles, less microtubule nucleation and less stabilization of microtubules by chromatin may explain why the density of microtubules between the chromosomes and the spindle poles falls.

Anaphase in the presence of nondegradable cyclin converts a spindle into two half spindles (Fig. 1*B* and ref. 5), suggesting that the linkage between sister chromatids maintains spindle bipolarity. Several mechanisms may stabilize the metaphase spindle. In each half of the spindle, the kinetochores stabilize bundles of microtubules running from the pole to the kinetochore. Because the two sister chromatids face in opposite directions, the linkage between them links the poles to each other via the kinetochore microtubules (reviewed in ref. 2). Microtubules that do not terminate at the kinetochore can be stabilized by poorly defined interactions with chromatin (reviewed in refs. 31 and 32). Finally, analyzing spindles with unreplicated chromosomes suggests that antiparallel interactions between microtubules nucleated at opposite poles of the spindle plays an important role in establishing and stabilizing bipolarity (13). Once sister chromatids separate and move apart, these stabilizing influences decline, microtubules ending in the center of the spindle depolymerize, and the spindle breaks in two. If the different microtubule-stabilizing mechanisms act synergistically, the metaphase spindle would be quite stable but would rapidly break down as sisters separate. Anaphase B still occurs in cells whose spindles lack chromosomes (D. Zhang and B. Nicklas, personal communication) suggesting that there are chromosome-independent mechanisms that allow the spindle to respond to changes in MPF activity.

Anaphase A and Poleward Microtubule Flux. During both metaphase and anaphase, marks made on microtubules move toward the spindle pole [polewards flux (23, 33)]. In kinetochore microtubules, flux occurs because microtubule depolymerization at the spindle pole is balanced by polymerization at the kinetochore making the individual subunits of the microtubule (the microtubule lattice) move to the pole. What is the relationship between flux and anaphase chromosome movement? During the initial stages of anaphase in tissue culture cells, chromosomes move toward the poles three to six times faster than marks made on kinetochore microtubules (23, 34). We have not measured flux and chromosome movement simultaneously for the spindles in *Xenopus* extracts, but chromosome movement in anaphase A (2.4 μm/min) occurs at about the rate of poleward microtubule flux in metaphase *Xenopus* spindles (12). This similarity suggests that anaphase A in early embryos may be driven entirely by poleward flux. However, since flux measurements in *Xenopus* spindles are dominated by nonkinetochore microtubules, this conclusion rests on the untested assumption that flux occurs at the same rate in kinetochore and nonkinetochore microtubules.

Following anaphase in individual spindles in cell extracts has revealed phenomena that were not easily seen in intact cells. This approach will greatly increase the range of experiments on spindle behavior that are accessible to real-time observation and should ultimately enable us to reconstitute functional spindles from purified components.

We thank the Marine Biological Laboratory, Nikon Inc., Universal Imaging Inc., the Program in Architectural Dynamics, and Shinya and Ted Inoue for their support for this collaborative project. Liz Blanton and Paul Maddox provided expert assistance for data analysis and digital photography. We are grateful to Cori Bargmann, Tim Mitchison, David Morgan, and Claire Waterman-Storer for their insightful comments on the manuscript. This work was supported by a Marine Biological Laboratory Nikon Fellowship to A.W.M., a Marine Biological Laboratory Rand Fellowship to E.D.S., and grants from the National Institutes of Health (to A.W.M. and E.D.S.) and the Packard Foundation (to A.W.M). A.B.D. is a predoctoral fellow of the Howard Hughes Medical Institute.

1. Wilson, E. B. (1928) *The Cell in Development and Heredity* (Macmillan, New York), 3rd Ed.
2. Inoue, S. & Salmon, E. D. (1995) *Mol. Biol. Cell* **6,** 1619–1640.
3. Murray, A. & Hunt, T. (1993) *The Cell Cycle: An Introduction* (Oxford Univ. Press, New York).
4. Shamu, C. E. & Murray, A. W. (1992) *J. Cell Biol.* **117,** 921–934.
5. Holloway, S. L., Glotzer, M., King, R. W. & Murray, A. W. (1993) *Cell* **73,** 1393–1402.
6. Belmont, L. D., Hyman, A. A., Sawin, K. E. & Mitchison, T. J. (1990) *Cell* **62,** 579–589.
7. Verde, F., Dogterom, M., Stelzer, E., Karsenti, E. & Leibler, S. (1992) *J. Cell Biol.* **118,** 1097–1108.
8. Karsenti, E., Kobayashi, S., Mitchison, T. & Kirschner, M. (1984) *J. Cell Biol.* **98,** 1763–1776.
9. Lohka, M. J. & Masui, Y. (1983) *Science* **220,** 719–721.
10. Lohka, M. & Maller, J. (1985) *J. Cell Biol.* **101,** 518–523.
11. Murray, A. W. & Kirschner, M. W. (1989) *Nature (London)* **339,** 275–280.
12. Sawin, K. E. & Mitchison, T. J. (1991) *J. Cell Biol.* **112,** 941–954.
13. Sawin, K. E. & Mitchison, T. J. (1991) *J. Cell Biol.* **112,** 925–940.

14. Sagata, N., Watanabe, N., Vande Woude, G. F. & Ikawa, Y. (1989) *Nature (London)* **342,** 512–518.
15. Watanabe, N., Hunt, T., Ikawa, Y. & Sagata, N. (1991) *Nature (London)* **352,** 247–248.
16. Salmon, E. D., Inoue, T., Desai, A. & Murray, A. W. (1994) *Biol. Bull.* **187,** 231–232.
17. Sullivan, K. M., Busa, W. B. & Wilson, K. L. (1993) *Cell* **73,** 1411–1422.
18. Ito, S., Dan, K. & Goodenough, D. (1981) *Chromosoma* **83,** 441–453.
19. Murray, A. W., Solomon, M. J. & Kirschner, M. W. (1989) *Nature (London)* **339,** 280–286.
20. Surana, U., Amon, A., Dowzer, C., McGrew, J., Byers, B. & Nasmyth, K. (1993) *EMBO J.* **12,** 1969–1978.
21. Verde, F., Berrez, J. M., Antony, C. & Karsenti, E. (1991) *J. Cell Biol.* **112,** 1177–1187.
22. Hiramoto, Y. & Nakano, Y. (1988) *Cell Motil. Cytoskeleton* **10,** 172–184.
23. Mitchison, T. J. & Salmon, E. D. (1992) *J. Cell Biol.* **119,** 569–582.
24. Paschal, B. M., Shpetner, H. S. & Vallee, R. B. (1987) *J Cell Biol* **105,** 1273–1282.
25. Endow, S. A., Kang, S. J., Satterwhite, L. L., Rose, M. D., Skeen, V. P. & Salmon, E. D. (1994) *EMBO J.* **13,** 2708–2713.
26. Aronson, J. F. (1971) *J. Cell Biol.* **51,** 579–583.
27. Blangy, A., Lane, H. A., d'Herin, P., Harper, M., Kress, M. & Nigg, E. A. (1995) *Cell* **83,** 1159–1169.
28. Sawin, K. E. & Mitchison, T. J. (1995) *Proc. Natl. Acad. Sci. USA* **92,** 4289–4293.
29. Karsenti, E., Newport, J., Hubble, R. & Kirschner, M. (1984) *J. Cell Biol.* **98,** 1730–1745.
30. Kuriyama, R. & Borisy, G. G. (1981) *J. Cell Biol.* **91,** 822–826.
31. Vernos, I. & Karsenti, E. (1996) *Curr. Opin. Cell Biol.* **8,** 4–9.
32. Waters, J. C. & Salmon, E. D. (1995) *BioEssays* **17,** 911–914.
33. Mitchison, T. J. (1989) *J. Cell Biol.* **109,** 637–652.
34. Zhai, Y., Kronebusch, P. J. & Borisy, G. G. (1995) *J. Cell Biol.* **131,** 721–734.